

## MODELLING OF THE DIE WEAR IN THE HOT FORGING PROCESS USING THE ARCHARD MODEL

MAREK WILKUS<sup>1\*</sup>, SŁAWOMIR POLAK<sup>2</sup>, ZBIGNIEW GRONOSTAJSKI<sup>2</sup>, MARCIN KASZUBA<sup>2</sup>,  
ŁUKASZ RAUCH<sup>1</sup>, MACIEJ PIETRZYK<sup>1</sup>

<sup>1</sup>AGH University of Science and Technology, al. Mickiewicza 30, 30-059 Kraków, Poland

<sup>2</sup>Wrocław University of Technology, Łukaszczyka 5, 50-371 Wrocław, Poland

\*Corresponding author: mwilkus@agh.edu.pl

### Abstract

In hot forging, die wear is the main cause of failure and cost of dies is a meaningful part of the manufacturing costs. In this paper, the wear analysis of a closed hot forging die used at the final stage of a component manufacturing has been performed. The simulation of forging process was carried out by commercial finite element software and the depth of wear was evaluated using Archard model. The results of the die wear measurements were used for identification of material parameters in the die wear model. Changes of the material parameter and hardness of the die material with increasing number of forgings were introduced in the model. By comparing the numerical results with measurements taken from the worn die, the accuracy of the model was evaluated for different points of the die surface. The parts of the die in which other than abrasive wear mechanism are active were identified.

**Key words:** Forging, tool wear, Archard model, identification

## 1. INTRODUCTION

In hot forging processes, the factors affecting die life are thermal fatigue, plastic deformation and wear. Among these, wear is the main failure cause in hot forging dies and cost of dies is a meaningful part of the manufacturing costs. It is estimated that the costs of the tools may amount to as much as 8–15% of the total production costs. Actually, if the time needed to replace the worn out tooling are accounted for, the costs may increase even further. Evaluation of various components of costs in a typical hot forging shop is shown in figure. 1. Moreover, tool wear significantly contributes to deterioration in the quality of the produced forgings. Basic information on wear can be found in (Bayer, 2004) and a review of the degradation mechanisms in forging tools was presented by Gronostajski et al. (2014a). The most common forging defects caused by tool wear are die cavity filling

errors, i.e. under-filling, laps, burrs, distortions, scratches, delamination and micro- and macro-cracks. The defects affect the functionality of the end product made out of the forging. Manufacturers of die forged products make efforts to reduce their costs and improve the quality of the forgings, eg. (Behrens et al., 2009; 2012). Numerical modelling of the tool wear can be helpful in reaching this goal.

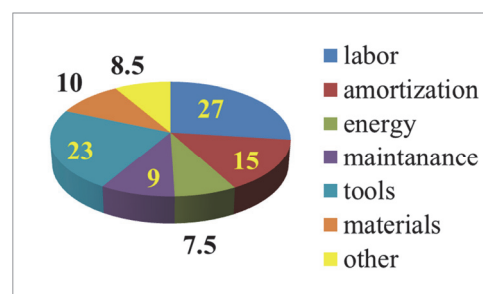


Fig. 1. Evaluation of various components of costs (percentage) in a typical hot forging shop.

Problem of wear of tool steels has been widely investigated in several laboratories, see research on the effect of temperature (Kocańda & Marciniak, 1990; Mozgovoy et al., 2009) or on the effect of heat treatment and surface quality (Jeong et al., 2001) or more global analysis of various aspects of the tool wear (Kocańda, 2003; Lavtar et al., 2011). All these studies were focused on fundamental understanding pertaining to the tribological characteristics of pre-hardened hot work tool steel during sliding against material of forgings. Less research have been performed on the analysis of the die wear in the industrial conditions, in particular on identification of the tool wear models and improvement of the accuracy of prediction of the tool wear. Turk et al. (2004) applied neural networks to create a large database on tools for hot forging, which was necessary for successful prediction of wear at a given number of strokes.

ber of forgings is not linear. Kang et al. (1999) and Gronostajski et al. (2013) accounted for the changes of the hardness of the tool steel during the process. This paper is focused on further analysis of the die wear during hot forging and evaluation of the material parameter in this model was the main objective of research. Finite element simulations of selected forging processes were performed and die wear was calculated. The results of the die wear measurements were used for identification of material parameters in the die wear model.

## 2. NUMERICAL MODEL

The commercial finite element code Forge with implemented Archard (1953) wear model was used to simulate the hot forging process. Details of this model are given below.

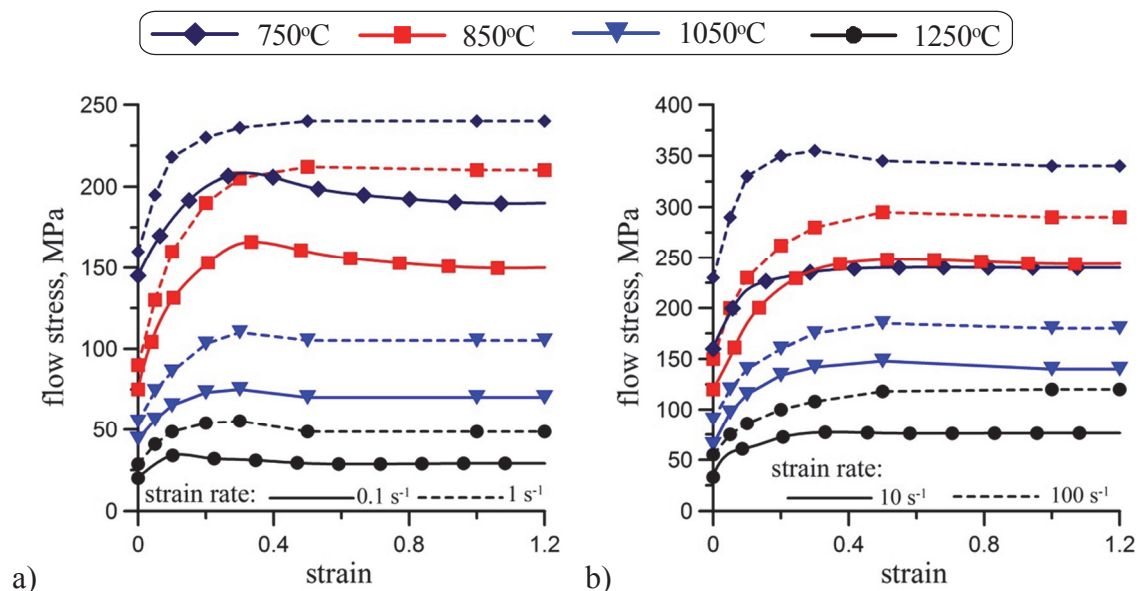


Fig. 2. Flow stress of the forged material: a) strain rates 0.1 and 1 s<sup>-1</sup>; b) strain rates 10 and 100 s<sup>-1</sup>.

In the last decade, many codes have been developed for computer simulation of solid-state metal forming and by means of these codes, 3D simulation of forging process has been possible, see papers (Abachi et al., 2009) for finite volume (FV) method and (Skóra et al., 2013) for the finite element (FE). The numerical simulation allows avoiding long and expensive experiments. Die wear models are implemented in the FE codes and local analysis of the wear is possible. Problems with determination of the material parameter in the die wear model are the main reason of difficulties with obtaining accurate and reliable results. Increase of wear with the num-

### 2.1. Finite element analysis of forging process

The finite element (FE) code Forge based on the Norton-Hoff visco-plastic flow rule (Norton, 1929; Hoff, 1954) was used in simulations. The constitutive law in Forge is (Chenot & Bellet, 1992):

$$\sigma = 2K \left( \sqrt{3} \dot{\epsilon}_i \right)^{m-1} \dot{\epsilon} \quad (1)$$

where:  $\sigma, \dot{\epsilon}$  - stress and strain rate tensors, respectively,  $K$  - material parameter, which is a function of the flow stress  $\sigma_p$ ,  $m$  - material parameter, which controls the balance between Newtonian liquid be-



haviour ( $m = 1$ ) and purely rigid-plastic behaviour ( $m = 0$ ).

Coulomb friction model with the friction coefficient of 0.35 for dry forging and 0.29 for lubricated process (Hensel, 1990) was used at the tool-forging interface. Flow stress  $\sigma_p$  of the forged material, which was C-Mn steel, was determined in the compression tests (figure 2). Relation of the flow stress on temperature, strain and strain rate was approximated by:

$$\sigma = A \exp(m_1 T) \varepsilon^{m_2} \dot{\varepsilon}^{m_3} \exp\left(\frac{m_4}{\varepsilon}\right) \quad (2)$$

Where:  $T$  – temperature in °C,  $\varepsilon$  - strain,  $\dot{\varepsilon}$  - strain rate, coefficients:  $A = 1327.34$ ,  $m_1 = -0.00257$ ,  $m_2 = -0.1941$ ,  $m_3 = 0.1468$ ,  $m_4 = -0.06521$ .

Mechanical model was coupled with the solution of the heat transfer equation:

$$\nabla \cdot k \nabla T + Q = c_p \rho \frac{\partial T}{\partial t} \quad (3)$$

where:  $k$  - conductivity,  $T$  – temperature,  $Q$  – heat generated due to plastic work,  $c_p$  – specific heat,  $\rho$  – density,  $t$  – time.

Neumann boundary condition was introduced at the tool-forging interface and at the free surfaces:

$$k \nabla T = \alpha (T_a - T) \quad (4)$$

where:  $T_a$  – ambient temperature or tool temperature,  $\alpha$  – heat transfer coefficient.

Heat transfer coefficient for a contact with the tool was  $\alpha = 25 \text{ W/m}^2\text{K}$ . Heat transfer coefficient for combined radiation and convection was assumed for free surfaces. Thermo physical properties and elastic modulus of the forged steel are given as a function of temperature in figure 3.

## 2.2. Die wear model

The wear process depends on many parameters that make it complicated for investigation. In the last decade, so many programs have been established for computer simulation of solid-state metal forming operations and by means of these developed programs, 3D simulation of forging process has been possible. From the very beginning of its applications to metal forming, the FE software is connected with models describing microstructure evolution, fracture, tool wear etc. In this paper, the analysis of die wear in forging is focused. The wear analysis was based on the Archard (1953) wear equation given as:

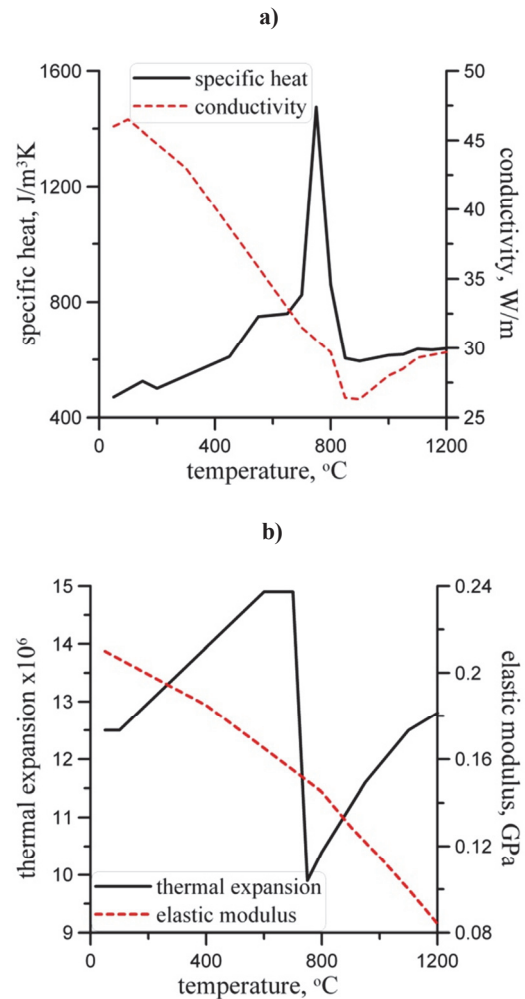


Fig. 3. Specific heat, conductivity (a), thermal expansion and elastic modulus (b) of the forged steel.

$$w = \int_0^t C \frac{\mu p v}{HV} dt \quad (5)$$

where:  $w$  – the depth of the wear calculated for one forging,  $C$  – the non-dimensional wear coefficient,  $\mu$  – friction coefficient,  $p$  – pressure normal to the die,  $v$  – slip velocity,  $HV$  – material hardness.

## 3. HOT FORGING PROCESS

Hot forging of the front wheel of the clutch in two operations was investigated. Details of this process are given in this section.

### 3.1. Description of the process

Forging process was composed of two operations (Gronostajski et al., 2014b). Cold rolled rods were cut into samples measuring  $\phi 75 \times 138 \text{ mm}$ . The first operation was upsetting. The upper and the lower die for this operation are shown in figure 4. Cross section of the lower die for the second forging



operation is shown in figure 5. Characteristic points, in which wear was analysed, are shown in figure 4b and in figure 5.

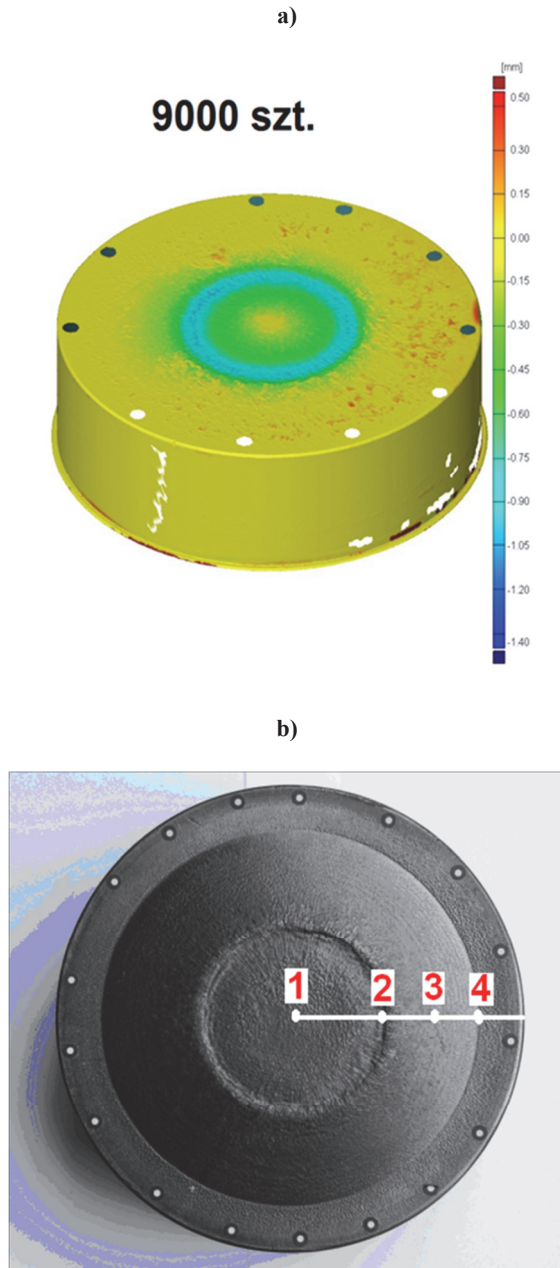


Fig. 4. Upper (a) and lower (b) die in the upsetting.

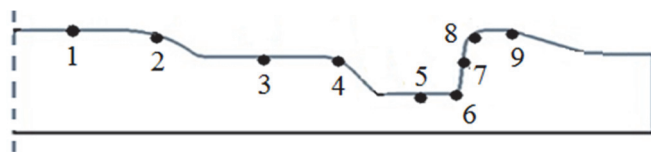


Fig. 5. Cross section of the lower die for the second operation in forging of the front wheel of the clutch.

Observations of the forging process allowed to draw some general conclusions, which were later used in the development of the model. Slip wear and

plastic deformation were main mechanism responsible for the tool wear. Some cracks occurred and were more pronounced in the 2<sup>nd</sup> operation than in the first one. These cracks were not seen after 550 forgings. After 6900 forgings cracks were seen in all parts of the die and small plastic deformation occurred around point 2 in figure 5. After 9000 forgings further cracks were seen in all parts of the die and plastic deformation occurred around points 1 and 2 in figure 5. Since lubrication was used in both operations, the Archard model was selected for the primary analysis.

### 3.2. Properties of the tool material

Material of the tool was steel X40Cr13 with the initial hardness of 46HRC in the state of the delivery before heat treatment. Thermo physical properties and elastic modulus of the forged steel are given as a function of temperature in figure 6.

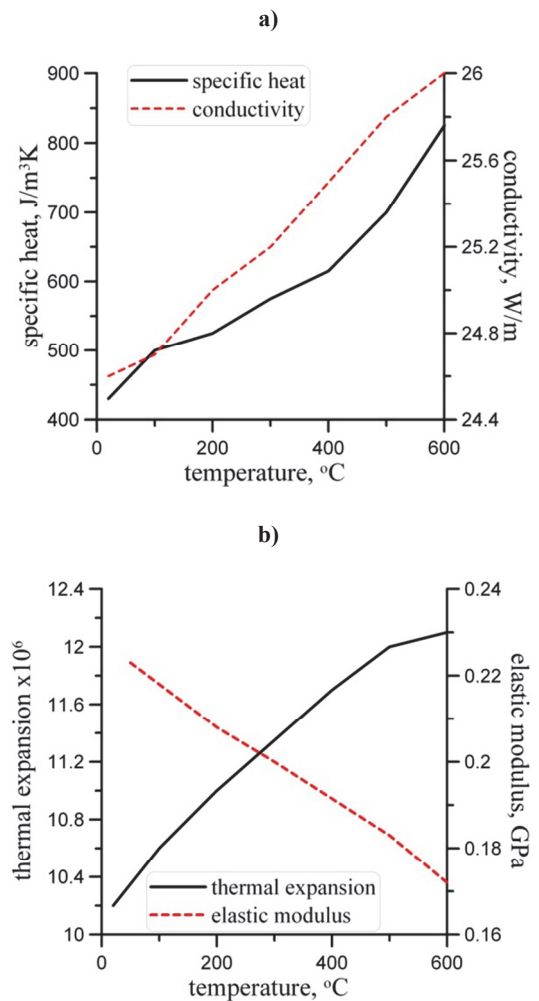


Fig. 6. Specific heat, conductivity (a), density and elastic modulus (b) of the tool material.

Specification of dies for the investigated processes is given in table 1. Hardness of new dies after



heat treatment was measured at selected points of the surface and the average values are given in table 1. Analysis of results shows large difference of the initial hardness. They were due to the fact that the die in the second operation was subject to nitriding, which resulted in large hardness. Application of lubricant was the second difference between the 2 operations. Lubrication resulted in a decrease of the friction coefficient but, on the other hand, it caused increase of the temperature variations during forging.

**Table 1.** Specification of dies for the investigated processes (C – clutch, Y – yoke).

operation	hardness HV	surface treatment	lubrication
C1 top	540	-	not lubricated
C1 bottom	540	-	not lubricated
C2 top	1100	nitriding	lubricated
C2 bottom	1100	nitriding	lubricated
Y top	540	-	lubricated
Y bottom	540	-	lubricated

Before forging material was heated to 1150°C. Temperature of the tool was 550°C. Process was performed in two operations, upsetting and forging. Dies were subject to the analysis after forging of 550, 1900, 6000 and 9000 of pieces. Hardness of the dies was measured at selected points of the die. Results of all measurements for various locations at the two dies and for various number of forgings are shown in figure 7. Analysis included microhardness measurements and scanning of the surface of the die. Microhardness distribution was measured using LECO–LM 100 AT instrument with the applied load of 0.1 kg for the time of 10 s. Scanning of the die surface was made using optical scanner GOM ATOS II.

In the first operation the dies were not subjected to nitriding and the drop of the hardness with increasing load was approximated by the two linear functions:

$$\begin{aligned}
 HV &= -587.7w + 476.5 && \text{for } w < 0.4 \text{ mm} \\
 HV &= 314.5 && \text{for } w \geq 0.4 \text{ mm}
 \end{aligned}
 \tag{6}$$

Analysis of the hardness measurements showed that the hardness decreases rapidly at the beginning of the wear, up to the value of about  $w = 0.37$  mm. Above this value hardness remains on the reasonably stable level. The following equations were used to

approximate relation of the hardness on the wear in the second operation:

$$\begin{aligned}
 HV &= -1827w + 979 && \text{for } w < 0.4 \text{ mm} \\
 HV &= 400 && \text{for } w \geq 0.4 \text{ mm}
 \end{aligned}
 \tag{7}$$

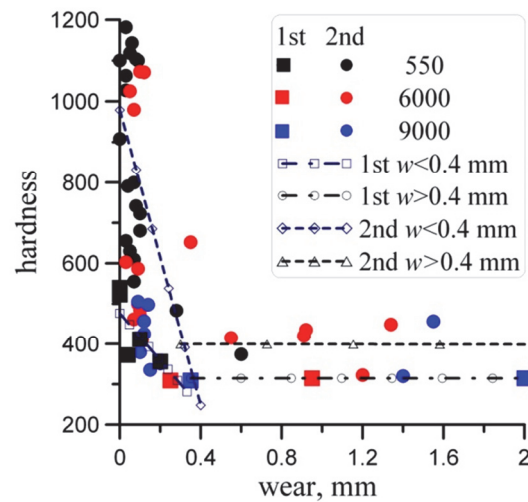


**Fig. 7.** Hardness vs wear measured at various locations of the two investigated dies after different numbers of forgings.

Results of measurement of the maximum wear of the top and bottom die after different numbers of forgings in upsetting are shown in figure 8. It is seen in this figure that the slope of both curves increases rapidly after forging of about 7000 of pieces. This result should be correlated with the microhardness measurements shown in figure 7. Although the results of micro hardness measurements are not consistent, the general tendency of decrease of hardness at the surface with increasing number of forging is observed.

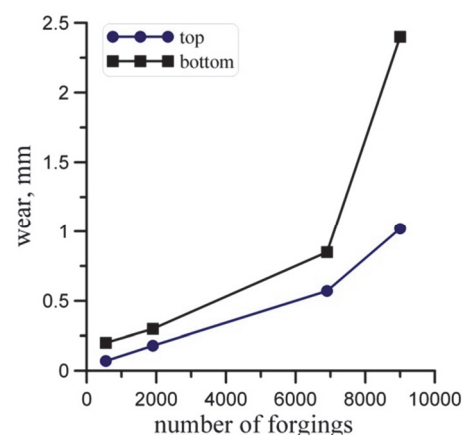


**Fig. 8.** Measurements of the maximum wear after different numbers of forgings.

It is known that in the closed die forging die wear results in lower stresses in the material and at the die-workpiece interface. To evaluate this effect simulations of forging in the die in figure 5 were



performed for a new die and for the die after 9000 forgings. Figure 9 shows comparison of forces for the two dies. It is seen that lower forces were predicted for the worn die. The difference is small at the beginning of forging and it increases rapidly at the final stage. This difference will be accounted for in simulations of die wear in industrial forging processes.

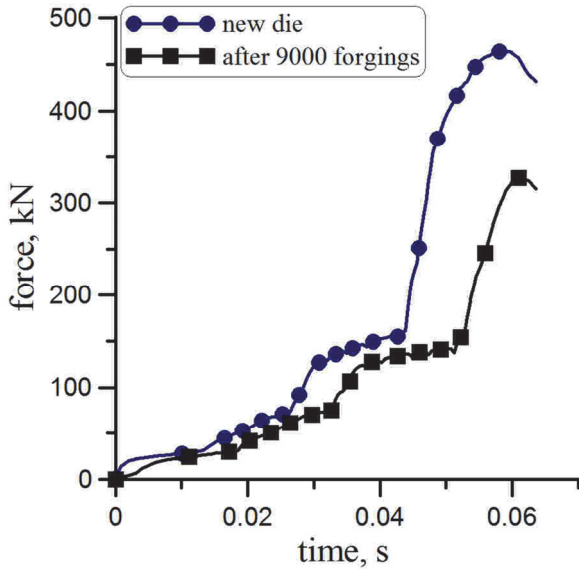


Fig. 9. Calculated loads for forging in a new die and in a die after 9000 forgings.

4. NUMERICAL SIMULATION

All simulations were performed using Forge FE code with the Archard (1953) tool wear model. First operation (upsetting) was used for identification of the tool wear model and the second operation was used for verification and validation of this model.

4.1. Upsetting – identification of the tool wear model

Simulations of the upsetting process were performed first. Selected results of calculated distribution of displacements in the radial and vertical directions are shown in figure 10. Distributions of strains, stresses and temperatures at the end of upsetting are shown in figure 11. These results confirm basic knowledge about the forging process, namely:

- Zone with very low strains (dead zone) occurs under the centre of the die and strains increase towards the edge of the forging.
- According to the yield criterion distribution of the effective strain resembles distribution of strains.
- Some temperature increase due to deformation heating is observed.

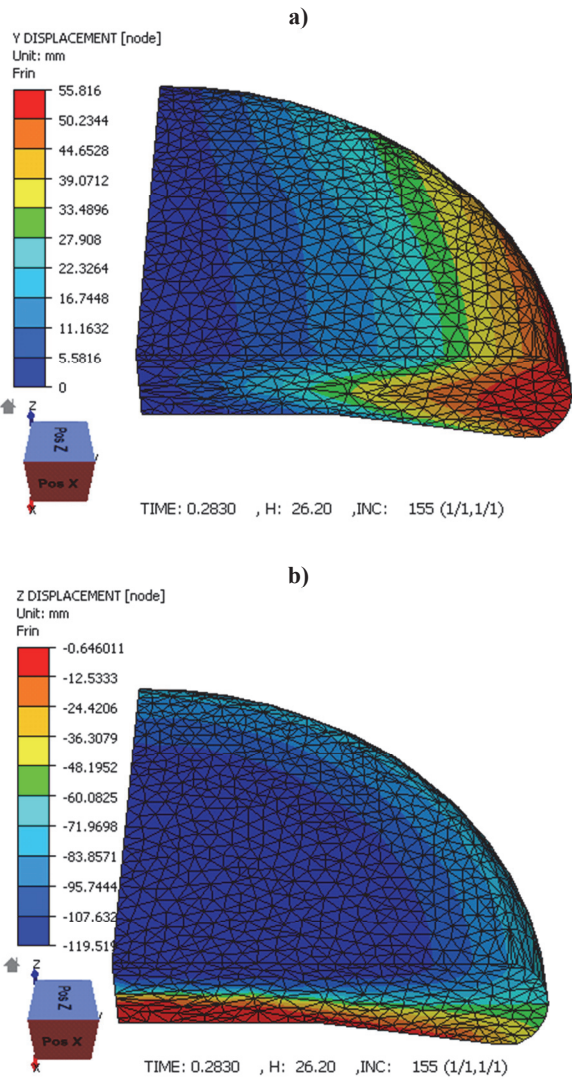


Fig. 10. Calculated displacements in upsetting in the Y (radial in the cutting plane) (a) and Z (vertical) directions (b).

Results of measurement of the wear distribution along the radius of the die were compared with the results of calculations. Analysis of results has shown that up to the certain threshold wear dependence on the number of forging  $w = w(N)$  is linear. When this threshold is exceeded the slope of this function increases, see figure 8. Therefore, the following values of the parameter  $C$  in equation (5) were proposed:  $C = 0.403 \times 10^{-4}$  for  $w \leq 4.9$  and  $C = 0.536 \times 10^{-4}$  for  $w > 4.9$ . Calculations with the optimized parameter  $C$  were performed next and comparison between measurements of the die wear distribution after different numbers of forgings and calculations using optimized model were made, see figure 12 for the top and bottom die in the first operation.



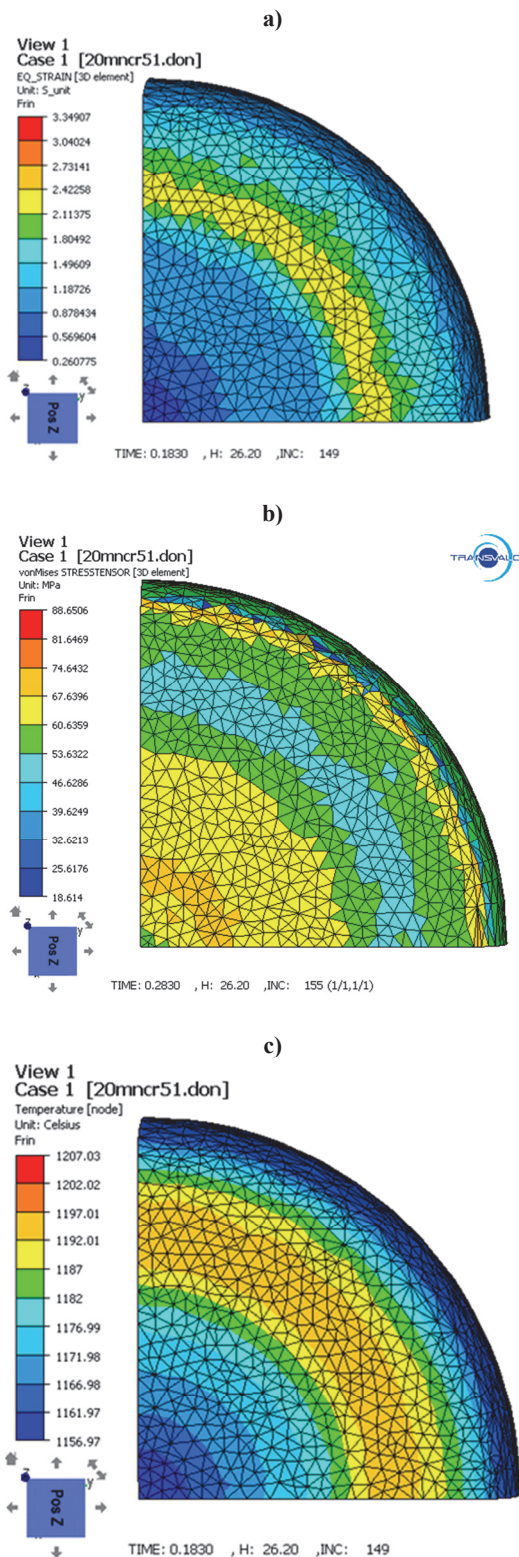


Fig. 11. Selected results of calculated distribution of the effective strain (a), effective stress (b) and temperature (c) in the first operation of the forging of the front wheel of the clutch.

#### 4.2. Identification of the tool wear model

Determination of the parameter  $C$  in equation (5) is crucial for the accuracy of quantitative predictions of the tool wear. This is a very difficult task because of the dispersion and lack of consistency of the ex-

perimental results. Therefore, in a majority of solutions not much attention is made to accurate evaluation of the parameter  $C$  and equation (5) is used rather for comparison of various dies and processes than for the accurate quantitative prediction of the wear. In the present paper a proposition of the identification procedure was developed on the basis of the inverse analysis concept. Since the full inverse algorithm requires a large number of simulations of the process (Sztangret et al., 2012), the computing times in the case of hot forging would be very long.

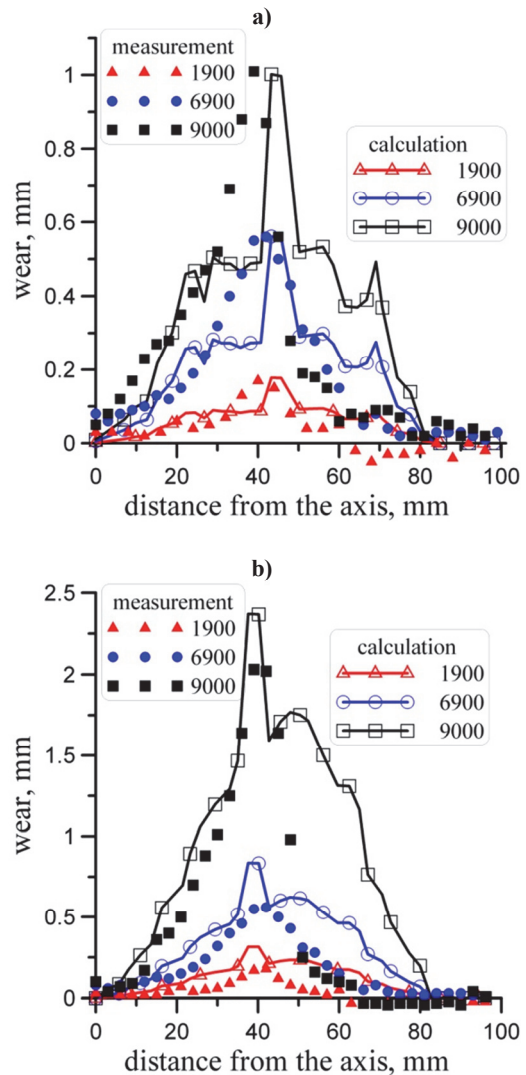


Fig. 12. Comparison of measurements of the die wear distribution after different numbers of forgings with calculations using model with the optimized parameter  $C$  in equation (5); a) top die, b) bottom die.

Each evaluation of the cost function in the inverse analysis would require finite element simulation of the forging process. Therefore, a simplified approach was proposed in which FE simulation was performed only once and inverse calculations were performed as the post processing operation. Calculated changes of the product of the normal pressure  $p$



and the distance of the slip  $\Delta u$  was the main output from the FE calculations. Results of these calculations for the die shown in figure 5 are presented in figure 13. To make this figure clear the points with a very small slip are not shown.

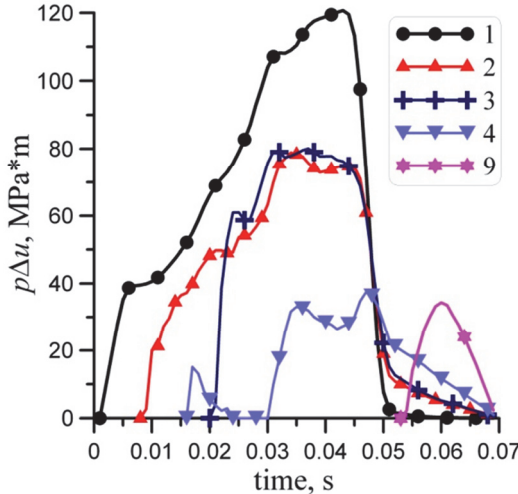


Fig. 13. Calculated changes of the product of normal pressure and distance of the slip for the points of the die shown in figure 5.

During simulation plots in figure 13 were integrated and the total work of the tangent stresses was calculated as:

$$W_{\tau} = \int_0^t \mu p v dt \quad (8)$$

Results of these calculations for all points distinguished in figure 5 are shown in figure 14. These values were further used for the calculation of the tool wear for various number of forgings  $N$ , using the formula:

$$w_{calc} = \sum_{i=1}^N \frac{W_{\tau}}{HV(w_{mi})} \quad (9)$$

In equation (9) work of the tangent stresses was divided by the current tool hardness, which was calculated from equation (7) using the tool wear from the experiment  $w_m$ .

Finally, the parameter  $C_i$  for a given number of forgings was calculated as the ratio of the measured wear  $w_{mi}$  and wear  $w_{ci}$  calculated from equation (9):

$$C_i = \frac{w_{mi}}{w_{ci}} \quad (10)$$

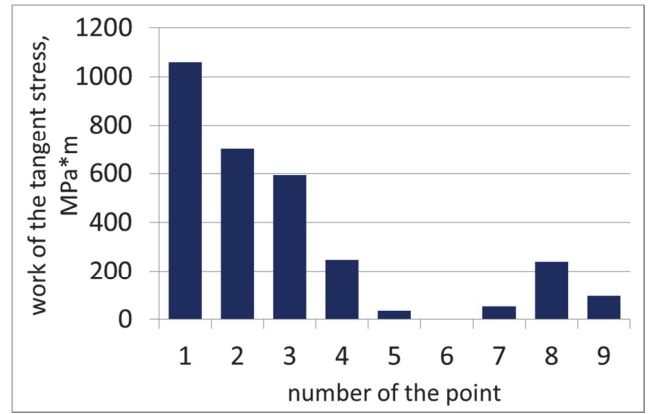


Fig. 14. Calculated total work of the tangent stresses for the points distinguished in the die in figure 5.

### 4.3. Forging – verification of the tool wear model

Simulations of the forging process were performed next. As it was done for the first operation, again selected results of calculated distribution of displacements in the radial and vertical directions are shown in figure 15. Distributions of strains, stresses and temperatures at the end of forging are shown in figure 16. Concentrations of strains and stresses are seen in the areas of large deformation

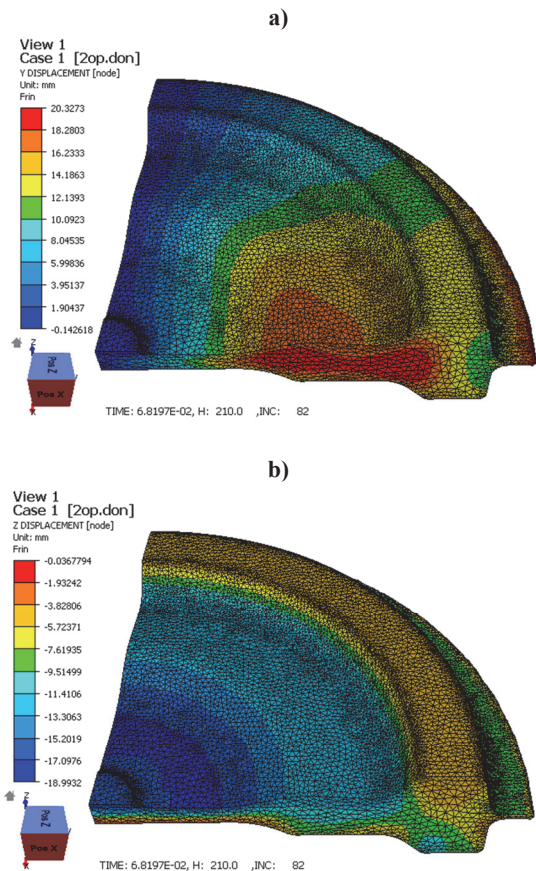


Fig. 15. Calculated displacements in upsetting in the Y radial in the cutting plane (a) and Z (vertical) directions (b) in the second operation of forging of the front wheel of the clutch.





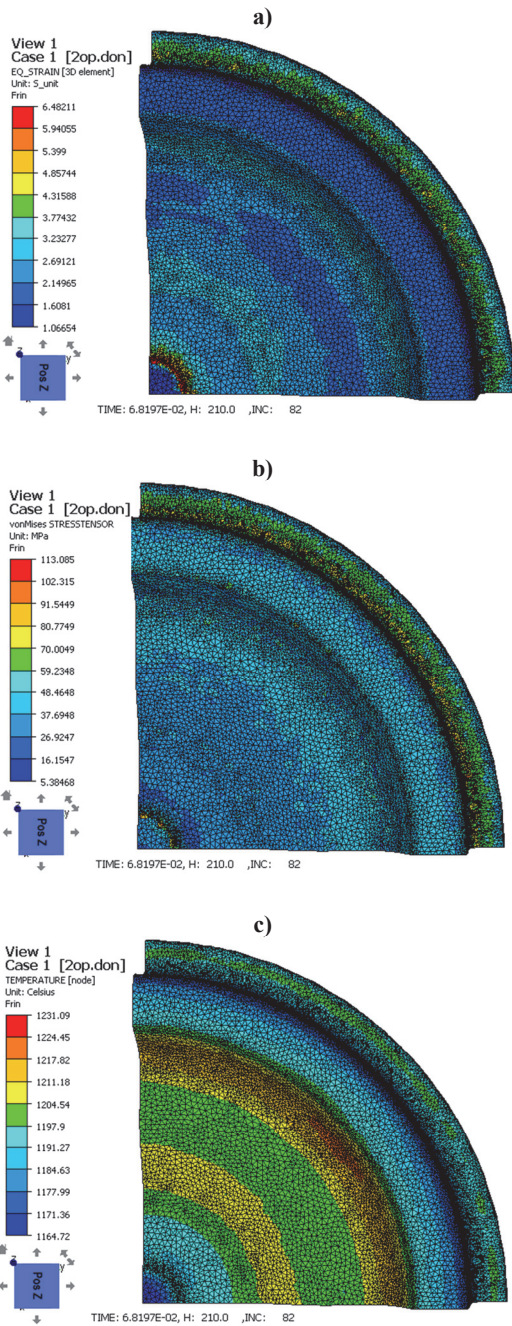


Fig. 16. Selected results of calculated distribution of the effective strain (a), effective stress (b) and temperature (c) in the second operation in forging of the front wheel of the clutch.

Values of the parameter  $C$  calculated from equation (10) for various numbers of forgings are presented as a function of the die wear in figure 17a. The results obtained for all points distinguished in figure 5 are presented. However, analysis of the results have shown the large discrepancies of the parameter  $C$  calculated for the points with a low value of the wear, therefore, these points are not shown in figure 17a. The level of the value of  $C$  parameter is comparable to the data published in the literature, see for example results obtained for simulation of hot forging process presented by Abachi et al. (2010), who reported the value of  $C/HV =$

$6.57 \times 10^{-7} \text{ MPa}^{-1}$ . Results of validation of the tool wear model with hardness calculated from equation (7) and with the parameter  $C$  calculated from equation (10) are shown in figure 17b. The agreement between measurements and calculations is not very good. It is probably due to the fact the global tool wear is an effect of various mechanisms, such as abrasive wear, oxidization, thermomechanical fatigue and plastic deformation, as well as the interdependences between them (Gronostajski et al., 2014). In spite of this complexity of the wear mechanism, beyond large discrepancies at the beginning of the process the general tendency of the wear was reproduced reasonably well in figure 17b.

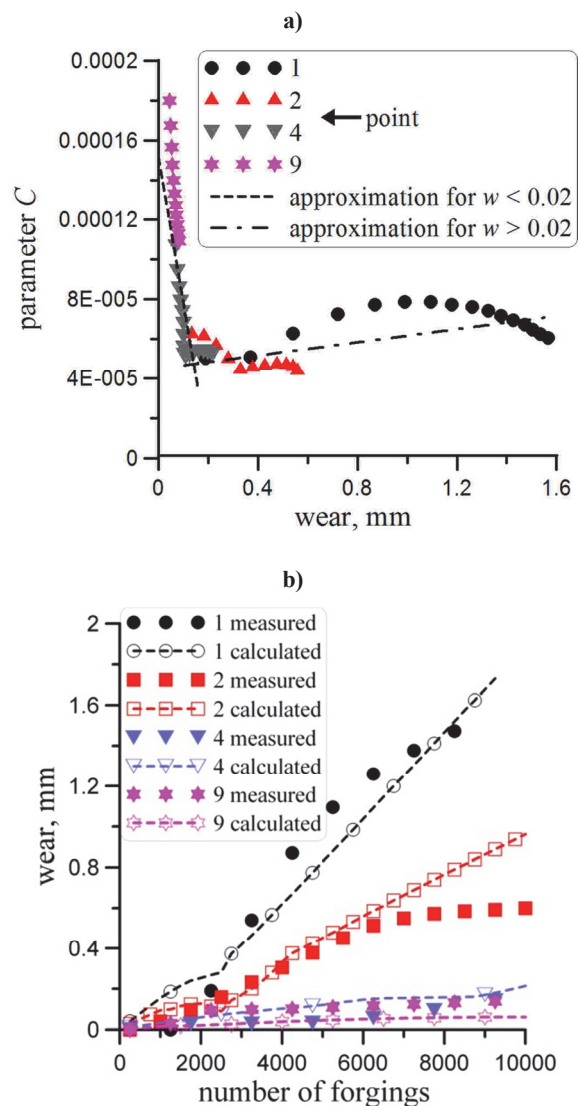


Fig. 17. Values of the parameter  $C$  calculated from equation (10) as a function of wear (a) and comparison of measured and calculated wear as a function of number of forgings.

Calculations of the die wear for the lower die in the second operation were performed with the optimized parameter  $C$  in equation (5). The values of the parameter  $C$  were those determined for the top die in



the first operation. Comparison between measurements of the die wear distribution after 9000 of forgings and calculations using optimized model were made, see results in figure 18. Comparison was made in the points marked in figure 5. Reasonably good agreement was obtained for all points except point 8. Since this point is located on the exposed part of the die, it is expected that other than sliding mechanisms cause an intensive wear observed in experiments. The model does not account for these mechanisms and failed to predict this intensive wear.

Accuracy of the model was not satisfactory for points 5 and 6, in which slip of the material with respect to the die was very small, see figure 14. In consequence the model predicted small wear in these points, while measured wear was larger. However, the largest discrepancy was observed in the point 8. Measured wear at that point was much larger than the predicted one. It is due to the fact that abrasive wear model does not describe properly the wear at that point. Probably other wear mechanism are involved what will be the objective of the research in the future.

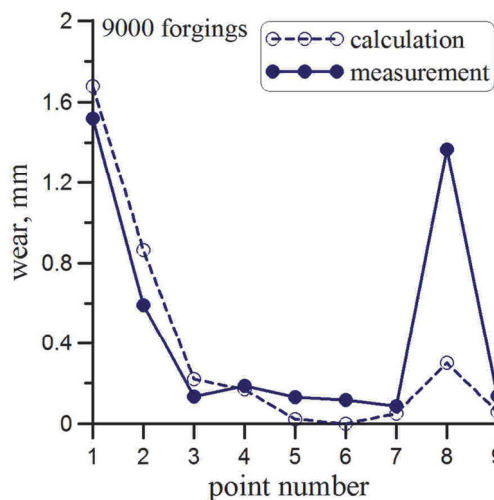


Fig. 18. Comparison of measurements of the die wear at various points with calculations using model with the optimized parameter  $C$  in equation (5) - bottom die in the second operation after 9000 of forgings.

## 5. CONCLUSIONS

Archard (1953) model gives reasonably good results when comparison of the tool wear due to slip between two processes is needed. Quantitative accuracy of this model requires determination of the parameter  $C$ , which is a difficult problem. A simplified procedure, which is based on one FE simulation of the process, was proposed in the paper. The following conclusions were drawn:

- Identification of the parameter  $C$  in the post processing, using results of the FE simulation performed only once, is possible. Work of the tangent stresses is calculated and it is used in the identification procedure.
- Large discrepancies in the value of  $C$  were observed at the beginning of the process for small values of the wear. More consistent values were obtained for larger number of forgings in these parts of the die, which were subjected to larger wear.
- In the closed die forging die wear causes decrease of pressure and, in consequence, it causes decrease of the work of frictional stresses. It was shown in the paper that this decrease can be meaningful. It means that the FE simulations should be repeated after every few thousands of forgings, accounting for the change of the shape of the die due to wear.
- Accounting for the changes of the tool hardness in predictions of the tool wear is crucial. The hardness drops rapidly at the beginning of the process and remains on a stable level for a larger number of forgings. The drop of the hardness is much larger for the dies with nitrided surface.
- Models of the tool wear based on one mechanism of wear only do not give quantitatively good results. It is suggested that hybrid models, which account for several mechanisms of wear, should be developed.

## ACKNOWLEDGEMENT

Work performed within the NCN project no. 2011/01/B/STB/02056.

## REFERENCES

- Abachi, S., Akkok, M., Gokler, M.I., 2010, Wear analysis of hot forging dies, *Tribology International*, 43, 467-73.
- Archard, J.F., 1953, Contact and rubbing of flat surfaces, *Journal of Applied Physics*, 24, 981-988.
- Bayer, R.G., 2004, *Mechanical Wear Fundamentals and Testing*, Marcel Dekker Inc., New York.
- Behrens, B.-A., Schäfer, F., 2009, Service life predictions for hot bulk forming tools, *Steel Research International*, 80, 887-891.
- Behrens, B.-A., Bouguech, A., Hadifi, T., Klassen, A., 2012, Numerical and experimental investigations on the service life estimation for hot-forging dies, *Key Engineering Materials*, 504-506, 163-168.
- Chenot, J.-L., Bellet, M., 1992, The viscoplastic approach for the finite-element modelling of metal forming



- processes, Numerical modelling of material deformation processes, (eds) Hartley, P., Pillinger, I., Sturges, C.E.N., Springer-Verlag, London, Berlin, 179-224.
- Jeong, D.J., Kim, D.J., Kim, J.H., Kim, B.M., Dean, T.A., 2001, Effects of surface treatment and lubricants for warm forging die life, *Journal of Materials Processing Technology*, 113, 544-550.
- Gronostajski, Z., Hawryluk, M., Niechajowicz, A., Zwierzchowski, M., Kaszuba, M., Bedza, T., 2011, Application of the scanning laser system for the wear estimation of forging tools, *Computer Methods in Materials Science*, 11, 425-431.
- Gronostajski, Z., Ziólkiewicz, S., Hawryluk, M., Kaszuba, M., Polak, S., Jaskiewicz, K., Będza, T., 2013, Modeling of the tool wear in TR forging of fastener, *Computer Methods in Materials Science*, 13, 77-83.
- Gronostajski, Z., Kaszuba, M., Hawryluk, M., Zwierzchowski, M., 2014a, A review of the degradation mechanisms of the hot forging tools, *Archives of Civil and Mechanical Engineering*, 14, 528-539.
- Gronostajski, Z., Będza, T., Kaszuba, M., Marciniak, M., Polak, S., 2014b, Modelling the mechanisms of wear in forging tools, *Obróbka Plastyczna*, 25, 301-315.
- Hensel, A., 1990, *Technologie der Metallformung -Eisen- und Nichteisenwerkstoffe*, Deutscher Verlag für Grundstoffindustrie.
- Hoff, N.J., 1954, Approximate analysis of structures in the presence of moderately large steps deformation, *Quarterly of Applied Mathematics*, 12, 49-55.
- Kang, J.H., Park, I.W., Jae, J.S., Kang, S.S., 1999, A study on die wear model considering thermal softening (II): Application of the suggested wear model, *Journal of Materials Processing Technology*, 94, 183-188.
- Kocańda, A., Marciniak, Z., 1990, On the problem of optimum temperature of warm working die, *CIRP Annals - Manufacturing Technology*, 39, 295-297.
- Kocańda, A., 2003, Określenie trwałości narzędzia w obróbce plastycznej metali, in: *Informatyka w Technologii Metali*, eds, Piela, A., Grosman, F., Kusiak, J., Pietrzyk, M., Publ.: Wydawnictwo Politechniki Śląskiej, Gliwice, 213-256 (in Polish).
- Lavtar, L., Muhič, T., Kugler, G., Terčelj, M., 2011, Analysis of the main types of damage on a pair of industrial dies for hot forging car steering mechanisms, *Engineering Failure Analysis*, 18, 1143-1152.
- Mozgovoy, S., Hardell, J., Deng, L., Oldenburg, M., Prakash, B., 2009, Effect of temperature on friction and wear of prehardened tool steel during sliding against 22MnB5 steel, *Tribology - Materials, Surfaces & Interfaces*, 8, 65-73.
- Norton, F.H., 1929, *Creep of steel at high temperature*, McGraw Hill, New York.
- Nowak, J., Węglarczyk, S., Pietrzyk, M., 2011, Numeryczna symulacja zużycia narzędzi w procesie kucia stopów na bazie miedzi z zastosowaniem różnych technologii kucia, *Archiwum Technologii Maszyn i Automatykacji*, 31, 77-91 (in Polish).
- Skóra, M., Węglarczyk, S., Pietrzyk, M., Numerical simulation of tool wear as support of optimization of manufacturing chain for fasteners, *Computer Methods in Materials Science*, 13, 2013, 68-76.
- Sztangret, Ł., Szeliga, D., Kusiak, J., Pietrzyk, M., 2012, Application of the inverse analysis with metamodelling for the identification of the metal flow stress, *Canadian Metallurgical Quarterly*, 51, 440-446.
- Turk, R., Peruš, I., Terčelj, M., 2004, New starting points for the prediction of tool wear in hot forging, *International Journal of Machine Tools and Manufacture*, 44, 1319-1331.

#### MODELOWANIE ZUŻYCIA NARZĘDZI DO KUCIA NA GORĄCO Z WYKORZYSTANIEM MODELU ARCHARDA

Streszczenie

W procesach kucia na gorąco zużycie narzędzi jest główną przyczyną ich zniszczenia i koszty narzędzi są znaczącą częścią całkowitych kosztów produkcji. W niniejszej pracy przeprowadzono analizę kucia w matrycach zamkniętych, stosowanego w końcowym etapie wytwarzania wyrobów kutych. Symulacje procesu kucia wykonano programem wykorzystującym metodę elementów skończonych połączoną z modelem Archarda i na podstawie tych symulacji określono wielkość zużycia ściernego. Wyniki pomiarów wielkości zużycia wykorzystano do identyfikacji parametrów materiałowych w modelu zużycia. Na podstawie porównania wyników obliczeń numerycznych z pomiarami matryc po odkuciu różnej liczby odkuwek oceniono dokładność modelu dla różnych punktów matrycy. Pozwoliło to na zidentyfikowanie obszarów matrycy, w których inne mechanizmy niż zużycie ściernie są odpowiedzialne za zużycie narzędzi.

Received: February 5, 2015

Received in a revised form: March 1, 2015

Accepted: March 23, 2015

